U.S. DEPARTMENT OF THE INTERIOR

U.S. GEOLOGICAL SURVEY

Results of Time-Domain Electromagnetic Soundings in Everglades National Park, Florida

by

David V. Fitterman, Maria Deszcz-Pan, and Carl E. Stoddard

Box 25046 MS 964
U.S. Geological Survey
Denver, CO 80225

Open-File Report 99-426

15 September 1999

ABSTRACT

This report describes the collection, processing, and interpretation of time-domain electromagnetic soundings from Everglades National Park. The results are used to locate the extent of seawater intrusion in the Biscayne aquifer and to map the base of the Biscayne aquifer in regions where well coverage is sparse. The data show no evidence of fresh, ground-water flows at depth into Florida Bay.

TABLE OF CONTENTS

LIST OF FIGURES

LIST OF PLATES

1. INTRODUCTION

A time-domain electromagnetic (TEM) sounding survey was made of Everglades National Park and surrounding areas to map salt-water intrusion, to obtain information about the Biscayne aquifer, and to look for evidence of fresh, ground-water flows to Florida Bay. This and other geophysical studies (Fitterman et al., 1995; Fitterman, 1996; Fitterman and Deszcz-Pan, 1998) are part of a larger effort by the U.S. Geological Survey and the Department of the Interior to study the South Florida Ecosystem (U.S. Geological Survey, 1997). The main focus of the work described in this report was to map saltwater intrusion, however, these data also proved important in removing calibration errors in helicopter electromagetic (HEM) surveys of the area (Deszcz-Pan et al., 1998).

The study area lies principally within Everglades National Park in southern Dade and Monroe Counties of south Florida (see Figure 1). The soundings were distributed so as to provide good areal coverage of the HEM survey flown in December 1994 (Fitterman and Deszcz-Pan, 1998).

A total of 36 soundings were made in August 1995 using a helicopter to reach the sounding locations. An additional 28 soundings were made between March and December 1996 at sites that were accessible by road.

2. HYDROGEOLOGY

Fish and Stewart (1991) have described the general framework of the hydrogeology of the eastern portion of the study area. Using cores recovered from boreholes, they mapped the surficial aquifer system. As only 12 of their wells are located in the study area, the coverage is limited, but adequate for developing a regional hydrogeologic model. The hydrogeology is characterized by three distinct zones, which from the surface to depth are the surficial aquifer system, the intermediate confining unit, and the Floridan aquifer system.

The Floridan aquifer system, because of its great depth (950 to 1000 ft, 290-305 m) in Dade County (Miller, 1986), is beyond the depth of exploration of our TEM measurements and need not be considered. Overlying the Floridan aquifer system is the intermediate confining unit consisting of a 550- to 800-ft (167-243 m) thick sequence of green clay, silt, limestone, and fine sand (Parker et al., 1955, p. 189). These sediments have relatively low permeability and produce little water.

The surficial aquifer system is composed, from top to bottom, of the Biscayne aquifer, a semiconfining unit, the Gray limestone aquifer, and the lower clastic unit of the Tamiami Formation. While the exact definition of the Biscayne aquifer has varied over the years, Fish and Stewart (1991, p. 12) define the Biscayne aquifer as being that part of the surficial aquifer system composed of

> "the Pamlico Sand, Miami Oolite, Anastasia Formation, Key Largo Limestone, and Fort Thompson Formation (all of Pleistocene age), and contiguous, highly permeable beds of the Tamiami Formation of Pliocene and late Miocene age. . . ."

Furthermore, Fish and Stewart require that there be at least a 10-ft (3-m) section of greater than 1000 ft/d (305 m/d) horizontal permeability for these units to be considered part of the aquifer. The base of the Biscayne aquifer is defined as the depth where the subjacent sands and clayey sands fail to meet this permeability criterion. In the study area the Biscayne aquifer ranges from 0 to 100 ft (0-30 m) thick; its thickness increases toward the east. The western extent of the Biscayne aquifer corresponds roughly with the north-south segment of highway SR 9336.

Below the Biscayne, a second aquifer composed of a gray limestone unit of the Tamiami Formation is found at depths of 70 to 160 ft (21-49 m) in western Dade County (Fish, 1988; Fish and Stewart, 1991). While less permeable than the Biscayne aquifer, the gray limestone aquifer is still significant, especially in the western portion of the study area where the Biscayne aquifer does not exist.

3. FIELD PROCEDURE

As most of the study areas is under 0.5 ft (0.15 m) to almost 6 ft (1.8 m) of water during the rainy season, working in the Everglades poses some operational problems, which are not usually encountered in surface geophysical studies. While, in general, sites were selected so as to provide a uniform distribution of stations, specific locations were selected based on the following criteria: ease and safety of helicopter landing, avoidance of hammocks (tree islands) and alligator holes and trails, avoidance of high density saw grass, and avoidance of deep water. Hammocks and trails were avoided for safety reasons. If the saw grass was too dense, it was impossible to walk through it. If the saw grass was too tall, navigating the straight lines required for the TEM transmitter loops was not possible. In deep water areas (greater than 2.5 ft (0.75 m)) the absence of saw grass meant that there was often nothing firm on which to walk.

The TEM transmitter and receiver must be kept dry to function properly. This was accomplished by floating them in plastic storage boxes. The receiver coil was perched on legs made from four-foot long wooden dowels. The transmitter loop was laid out in the form of a square with a side length of 40 m. Marks on the loop wire were used to measure distance, and a right-angle prism assured orthogonality of loop sides. Tall plastic poles were pushed into the ground at the corners of the loops to provide sighting targets. The receiver coil was located at the middle of the transmitter loop by sighting on the corner poles with the right-angle prism. The transmitter wire usually was strung over the saw grass or laid in the water where the grass was sparse. No adverse effects were noted from having the transmitter wire in the water except near Shark River Slough where deeper water was encountered and current leakage out of the transmitter wire may have been more pronounced. In general, a sounding could be completed in 1 to 1-1/2 hours.

A Geonics PROTEM EM47 system was used to make the measurements. After setting up the equipment and adjusting the transmitter current and receiver gain, six or seven measurements were made at base frequencies of 315 and 30 Hz, corresponding to time ranges of 6.8-701 μs and 0.1-7.0 ms, respectively.

4. DATA PROCESSING AND INTERPRETATION

The data from the various measurements were averaged and standard deviations computed. Voltages were converted to late-stage apparent resistivity using the standard formula (Kaufman and Keller, 1983; Spies and Eggers, 1986):

$$\rho_a^{LS} = \frac{\mu_0}{4\pi t}\left(\frac{2\mu_0 L^2 M_r I}{5 t V}\right)^{2/3} \qquad (1)$$

where μ_0 is the magnetic permeability of free space ($4\pi 10^{-7}$ H/m), t is the time since transmitter current turnoff, L is the side length of the square transmitter loop, M_r is the receiver coil turns-area product, I is the transmitter current, and V is the received voltage. All units are SI.

The computed percentage standard deviation typically ranged from 0.1 to 1 percent at times less than 0.7 ms. At times greater than 1 ms the percentage standard deviation increased to values from 1 to 15 percent. Data with apparent resistivity standard deviations greater than 10 percent were usually deleted before interpretation was begun. Data points which deviated from a smooth apparent-resistivity-time plot were also removed. Summaries of the averaged apparent resistivity data are given in Appendix 1.

The TEM response of layered earth models was computed and compared with the data using a commercially available program (TEMIX GL, Interpex Limited, 1993). In this process, called inversion, the model parameters (layer thicknesses and resistivities) were adjusted to reduce the average squared misfit error between the observed and computed responses. The philosophy used in inverting the data was to determine the model with the fewest layers whose response adequately fitted the data. If the data fit did not look satisfactory, additional layers were used, and the model resolution was checked. If the additional layers could be adequately resolved, they were retained; otherwise, the simpler model was used. The resulting models usually had three layers, though a few models had only two or four layers.

5. TYPICAL SOUNDINGS

Most of the TEM soundings fall into one of two types as shown in Figure 2. (Refer to Figure 1 for sounding locations.) Sounding EG111 has a slight initial descending branch between 0.007 and 0.06 ms, a nearly horizontal section from 0.1 to 0.4 ms, and a final descending branch after 0.5 ms. In contrast, sounding EG108 has significantly lower apparent resistivities, as well as a dramatic descending branch (0.007-0.2 ms), a pronounced minimum near 0.36 ms, and an ascending branch (0.6-4 ms). Figure 2b shows the inverted layer resistivities and thicknesses for the two soundings. The interpreted resistivities of soundings EG111 and EG108 behave in a fashion similar to their respective apparent resistivity curves. Sounding EG111 has a monotonic decrease in resistivity with depth, while sounding EG108 has a resistivity minimum.

While the data are modeled with sharp transitions between resistivity values, actual variations in pore water conductivity, geology, and formation resistivity, are likely to be transitional over a finite distance. This point should be kept in mind when using the TEM model results.

For the most part, all of the TEM soundings from our field work are characterized by these two examples. Plots for all of the soundings can be found in Appendix 2. In general, the apparent and interpreted resistivity are lower at locations nearer to the coast than for soundings further landward.

6. FORMATION RESISTIVITY-WATER QUALITY RELATIONSHIP

Borehole geophysical measurements from wells in the study area provide insight into the cause of the low interpreted resistivities found in some of the TEM soundings, such as the second layer of sounding EG108 mentioned previously. From induction logs, which measure formation resistivity, and measurements of water conductivity, both in the borehole and from samples pumped from the wells, the following relationship was established

$$SC = 81200\,\rho_f^{-1.062} \qquad (2)$$

where SC is the specific conductance in µS/cm and ρ_f is the formation resistivity in ohm-m. This relationship (see Figure 3) can be used to convert interpreted layer resistivity to SC of the saturating pore fluid.

Often chloride ion concentration is of interest to hydrogeologic modelers. To convert specific conductance to chloride ion concentration we use a relationship established for surface waters in south Florida shown in Figure 4 (A. C. Lietz, written commun., 1998). The specific conductivity increases nonlinearly with chloride concentration for chloride levels below 650 ppm. At higher chloride concentrations, the relationship becomes linear. Using the south Florida SC-Cl relation and equation (2), the ρ_f-Cl graph in Figure 4 was generated.

The chloride ion concentrations of fresh and saline ground waters are usually quite different resulting in large differences in formation resistivity for fresh and saline saturated geologic materials (Freeze and Cherry, 1979; Archie, 1942; Hearst and Nelson, 1985). The graph shown in Figure 4 provides a way of estimating chloride levels from inverted TEM data, however, it must be stressed that this relationship is based upon an assumption that ground water in the area has the same SC-Cl relationship as surface water. This is a reasonable assumption as the source of Cl is most likely from seawater for both ground and surface water. Because of its statistical nature there is some uncertainty in equation (2), and consequently in the formation-resistivity-chloride relationship. Nonetheless, this relationship is useful provided its limitations are understood.

In Figure 5 the interpreted layer resistivities of the first and second layers for all of the TEM inversion models are plotted as a function of depth to the bottom of the model layer. Most of the data separate into two clusters: those whose

resistivities are greater than 15 ohm-m and those whose resistivities are less than 10 ohm-m

The curve in Figure 4 indicates that formation resistivities of less than 10 ohm-m correspond to chloride levels of more than 2000 ppm. Taking this level as a separation point, the resistivity values of less than 10 ohm-m are interpreted to be saltwater saturated. The interpreted layer resistivity data are shown as box plots in Figure 6. This presentation shows that there is a wide range of resistivity values for the various layers, however, the average resistivity is lower in layer 2 than layer 1. The ratio of average resistivity of freshwater to saltwater saturated zones is 36 and 11 for layers 1 and 2, respectively.

7. DISCUSSION

7.1 Extent of Saltwater Intrusion

In Plate 1 is shown the location of all the TEM soundings. Some of the location symbols have a number associated with them indicating the depth to a resistivity of less than 10 ohm-m. Resistivities this low are associated with saltwater saturation as discussed previously. Also shown are Fish and Stewart's (1991) contours of depth to the base of the Biscayne aquifer. If the conductive layer (less than 10 ohm-m) is shallower than the base of the Biscayne, the site is considered to be saltwater intruded in the Biscayne. Based upon the locations of these points a line representing the freshwater/saltwater interface (FWSWI) was drawn. The density of TEM soundings is high enough to precisely control the location of the FWSWI except in the western part of the survey (near EG124 and EG126). In this region knowledge of the influence of the tidal rivers on the interface has been used in estimating the FWSWI location (Fitterman, 1996; Fitterman and Deszcz-Pan, 1998). The interface extends landward a great distance. At the southern extent of Taylor Slough (near EG120 and EG119) it is about 8-10 km inland. Near the bend in the C-111 canal between EG110 and EG223, the interface moves slightly further landward (10-12 km). West of Nine Mile Pond the interface's location is controlled by the numerous tidal rivers, which extend inland anywhere from 12 to 30 km.

7.2 Base of Biscayne Aquifer

Fish and Stewart (1991) constructed a map showing the depth to the base of the Biscayne aquifer. In Plate 2 their contours, and the 12 wells upon which the contours are based, are shown. In some parts of the map, where the distance between wells is large, the control on the contours is less reliable. For example, across the southern edge of the map the three wells (G3322, G3323, and G3395) used to draw the contours have spacings of 30-40 km between them. In an attempt to improve this situation, a map of the bottom of the Biscayne aquifer based on the TEM interpretations was made. A resistivity change is expected at the base of the Biscayne aquifer because of the difference in hydrologic properties between the Biscayne aquifer, the underlying semiconfining unit, and the gray limestone unit.

The map was constructed using the following criteria. First a map was made of the depth to the bottom of the first layer from TEM sounding landward of the FWSWI shown in Plate 1 to insure that the mapped layer was freshwater saturated. Points that were significantly greater than the Fish and Stewart contours were eliminated from the map. Sometimes the depth to the bottom of the second (or third) layer was used when the first (and second) layer was obviously too thin. Second, for soundings that were saltwater saturated, the depth to the base of the conductive layer was taken as the base of the Biscayne because the semiconfining unit at the base of the Biscayne is usually more resistive than the overlying layers. Again, the depths had to be comparable to the Fish and Stewart contours. Third, the data points were gridded and points which did not fit in smoothly with neighboring points were rejected. Incompatible points were often associated with soundings which had large misfit errors caused by noise from nearby power lines. Finally the retained data points were regridded to produce the final map shown in Plate 2.

The TEM-derived map shows a deepening of the Biscayne in the easterly direction. In general, this map is compatible with the drilling results of Fish and Stewart. Considering the sparse number of wells available to Fish and Stewart and the inherent errors in the TEM depth estimates (perhaps 10-15 percent of total depth), the data are remarkable similar. However, there are some differences. Fish and Stewart show a ridge in the surface starting near well G3319 in the bend of levee L31W, proceeding toward the intersection of the C-111 and C-111E canals, and continuing east of well G3324. The TEM-derived contours, on the other hand, show a basin west of Taylor Slough (EG215 and EG220) and a pronounced valley going from EG111 toward EG108 and EG106. The TEM-derived contours are more east-west oriented near Ingraham Highway, while the well-based contours are more north-south oriented.

7.3 Depth to Conductive Layer

In Plate 3 is shown a map of depth to a conductive layer based on the TEM sounding interpretations.

Several criteria were used in selecting the depth to the conductive layer from the TEM resistivity-depth (ρ-z) interpretations:

1. If a minimum exists in the ρ-z curve, the depth to the minimum resistivity is used. All minima are less than 10 ohm-m, with most less than 5 ohm-m, indicative of saltwater intrusion.

2. If the ρ-z curve decreases with depth, the depth where the resistivity become less than 10 ohm-m is selected.

3. If the ρ-z curve decreases with depth, but the resistivity is always greater than 10 ohm-m, the depth where it becomes less than 30 ohm-m is selected, provided there is a significant reduction in resistivity (factor of 2) from the overlying layer.

Soundings with poor data quality were not used. The selected points were gridded and examined. Data points that produced single point anomalies were eliminated.

The map depth of conductive layer map, shown in Plate 3, is geophysical by definition, but its behavior reflects several hydrogeologic features.

1. The depth to the conductive layer decreases in the seaward direction as a result of saltwater intrusion.
2. The contours deepen under Taylor Slough between EG121 and EG119 suggesting that Taylor Slough is a rather deep feature.
3. The contours deepen along the line of stations to the south of the dog-legged portion of the C-111 canal. This is interpreted as the result of flow through bank cuts along the south side of the canal, which existed at the time the TEM measurements were made. This flow recharges the aquifer and displaces saltwater.
4. An anomalously shallow region is seen between EG206, EG130, and EG207, which is thought to be due to saltwater intrusion from the north-west and from the south of this area. This interpretation is supported by the HEM data (Fitterman and Deszcz-Pan, 1998).

7.4 Freshwater Discharge to Florida Bay

Studies of the south Florida ecosystem have raised questions about the possible existence of fresh, ground-water flows to Florida Bay. If such flows exist, they could have a significant impact on the Florida Bay ecosystem.

From the TEM results discussed previously, it appears that the Biscayne aquifer is saltwater saturated from the FWSWI all the way to Florida Bay. This statement is based upon the location of the FWSWI as shown in Plate 1 and the depth to the conductive layer (see Plate 3). The presence of fresh, ground-water flows seaward of the FWSWI are expected to show up as zones with resistivities greater than 15 ohm-m.

A cross section was constructed from the TEM inversion results for the southern most soundings (Figure 7). For all of the soundings the resistivity is less than 10 ohm-m at depths of 10 m or less. In several cases, the low resistivity zone comes to the surface. These low resistivity zones is often thick. For several soundings (EG302, EG212, EG121, EG107, EG106, and EG105) the low resistivity zone extends to a depth in excess of 40 m. Only sounding EG119 has a thick, high resistivity (69 ohm-m) layer, which is associated with Taylor Slough. The slough also appears as a deep resistive feature in helicopter electromagnetic (HEM) data. The HEM data establish the southern extent of this feature near sounding EG119 (Fitterman and Deszcz-Pan, 1998). Some of the soundings have high resistivity surface layers (EG212, EG121, EG119, EG108, EG106, and EG105) that are likely freshwater saturated material.

The question of whether or not there are fresh, ground-water flows to Florida Bay becomes one of 1) whether or not the thin, high resistivity zones mentioned

above continue to Florida Bay, and 2) if these zones represent ground-water flows. Based on the geophysical data, the search for fresh, ground-water flows should focus on the upper 5 meters in the vicinity of the coast line.

The geophysical data rule out the possibility of thick zones of fresh, ground water south of the FWSWI. However, it is possible for thin, resistive zones to exist, which are not detectable by the TEM soundings. For example, if we consider the sounding taken near Flamingo (EG302), a 2-m thick resistive zone could exist at a depth of 15 m and not be detected. While allowed by the TEM data, other evidence, such as well logs, is required to support the existence of a thin, resistive layer.

8. CONCLUSIONS

The interpreted TEM measurements show a distinct range of layer resistivities, which correspond to freshwater and saltwater saturated materials. Based on this and the results of geophysical borehole measurements, the TEM results have been used to map the FWSWI. In addition to mapping the FWSWI, the TEM soundings provide a more detailed estimate of the depth to the base of the Biscayne aquifer than is possible from the limited number of existing wells. A depth to conductor map was also produced which shows the extent of saltwater intrusion as well as the deep resistive zone associated with Taylor Slough. These maps are of value in developing ground-water flow models of the area. TEM soundings show no evidence of freshwater saturated zones at depth. However, there appear to be high resistivity zones near the surface that could be due to fresh, ground-water flows. The search for flows should be focused on the upper 5 m in the coastal zone.

9. REFERENCES

Archie, G.E., 1942, The electrical resistivity log as an aid to determining some reservoir characteristics: Trans. AIME, v. 146, p. 54-62.

Deszcz-Pan, M., Fitterman, D. V., and Labson, V. F., 1998, Reduction of inversion errors in helicopter EM data using auxiliary information: Exploration Geophysics, v. 29, p. 142-146.

Fish, J.E., 1988, Hydrology, aquifer characteristics, and ground-water flow of the surficial aquifer system, Broward County, Florida: U.S. Geological Survey Water-Resources Investigations Report 87-4034, 92 p.

Fish, J.E., and Stewart, Mark, 1991, Hydrogeology of the surficial aquifer system, Dade County, Florida: U.S. Geological Survey Water-Resources Investigations Report 90-4108, 50 p., 11 plates.

Fitterman, D.V., Fennema, R.J., Fraser, D.C., and Labson, V.F., 1995, Airborne electromagnetic resistivity mapping in Everglades National Park, Florida, in Symposium on the Application of Geophysics to Engineering and Environmental Problems SAGEEP '95, Orlando, Florida, April 23-27, 1995, p. 657-670.

Fitterman, D. 1996, Geophysical mapping of the freshwater/saltwater interface in Everglades National Park, Florida, U.S. Geological Survey Fact Sheet FS-173-96.

Fitterman, D.V., and Deszcz-Pan, M., 1998, Helicopter EM mapping of saltwater intrusion in Everglades National Park, Florida: Exploration Geophysics, v. 29, p. 240-243.

Freeze, R.A., and Cherry, J.A., 1979, Groundwater: Englewood Cliffs, New Jersey, Prentice Hall, 604 p.

Hearst, J.R., and Nelson, P.H., 1985, Well logging for physical properties: New York, McGraw-Hill, 571 p.

Interpex Limited, 1993, TEMIX GL v. 3: Transient electromagnetic interpretation software, user's manual, 434 p.

Kaufman, A.A., and Keller, G.V., 1983, Frequency and Transient Sounding: Amsterdam, Elsevier, 685 p.

Miller, J.A., 1986, Hydrogeologic framework of the Floridan aquifer system in Florida and parts of Georgia, Alabama, and South Carolina: U.S. Geological Survey Professional Paper 1403-B, 91 p.

Parker, G.G., Ferguson, G.E., Love, S.K., and others, 1955, Water resources of southeastern Florida, with special interest to the geology and ground water of the Miami area: U.S. Geological Survey Water-Supply Paper 1255, 965 p.

Spies, B.R., and Eggers, D.E., 1986, The use and misuse of apparent resistivity in electromagnetic methods: Geophysics, v. 51, p. 1462-1471.

U.S. Geological Survey, 1997, U.S. Geological Survey Program on the South Florida Ecosystem – Proceedings of the Technical Symposium in Ft. Lauderdale, Florida, August 25-27, 1997: U.S. Geological Survey Open-File Report 97-385, 100 p.

FIGURE CAPTIONS

Figure 1 Map showing the location of TEM soundings.

Figure 2 Apparent resistivity data and model interpretation for two representative TEM soundings.

Soundings EG111 and EG108, which are located landward and seaward, respectively, of the FWSWI. Sounding locations are shown in Figure 1. Measured apparent resistivity data (avg) are plotted as symbols, while the calculated model results (cal) are plotted as lines. Vertical lines through the data points indicate the estimated uncertainty in the measurements. The data are collected using two transmitter repetition frequencies. The earlier time data are denoted as ultra high (uh), and the later time data are denoted as high (hi).

Figure 3 Scatter plot of formation resistivity as function of water specific conductance from wells in Everglades National Park.

The best fit power law through the data is shown.

Figure 4 Formation resistivity and water specific conductance as a function of chloride ion concentration.

Figure 5 Scatter plot of interpreted layer resistivities as a function of depth to bottom of layer.

Resistivities are coded for layer (rho1, rho2) and water quality (FW for freshwater, SW for saltwater).

Figure 6 Box plot of interpreted layer resistivities for freshwater and saltwater saturated zones.

FW and SW designate freshwater and saltwater, respectively. The number indicates the TEM model layer.

Figure 7 Cross section from soundings along southern edge of study area.

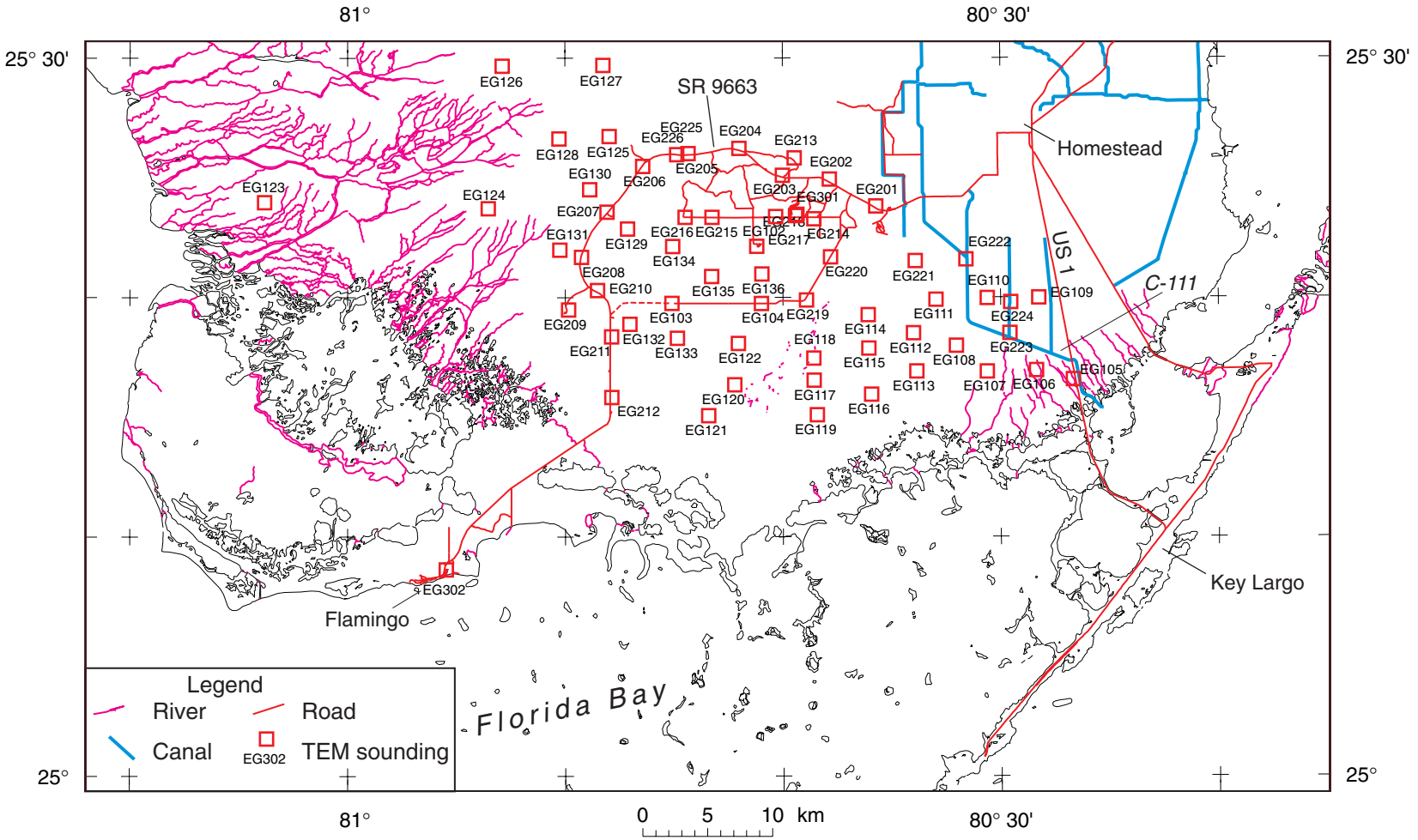

Figure 1 Map showing the location of TEM soundings.

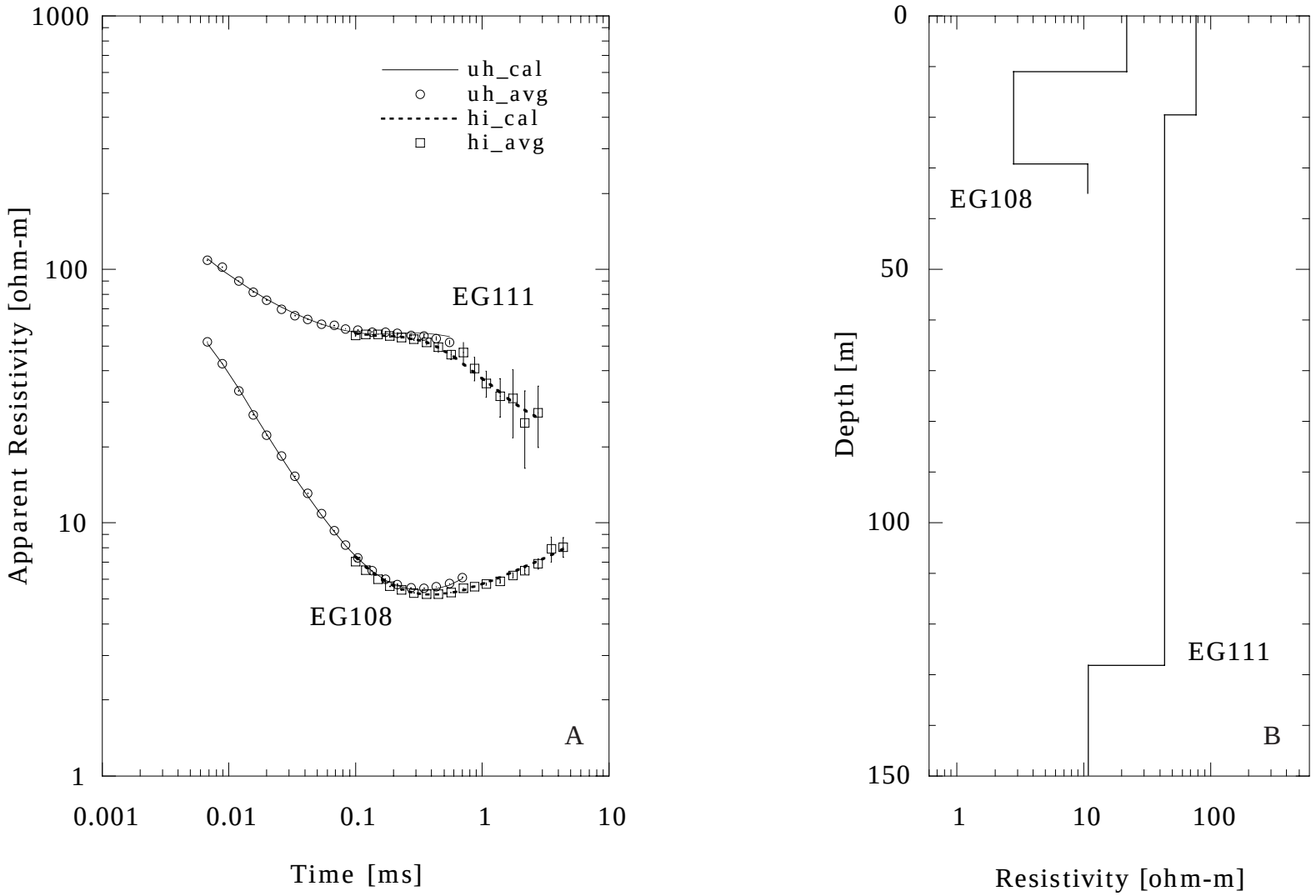

Figure 2 Apparent resistivity data (A) and model interpretation (B) for two representative TEM soundings. Soundings EG111 and EG108, which are located landward and seaward, respectively, of the FWSWI. Sounding locations are shown in Figure 1. Measured apparent resistivity data (avg) are plotted as symbols, while the calculated model results (cal) are plotted as lines. Vertical lines through the data points indicate the estimated uncertainty in the measurements. The data are collected using two transmitter repetition frequencies. The earlier time data are denoted as ultra high (uh), and the later time data are denoted as high (hi).

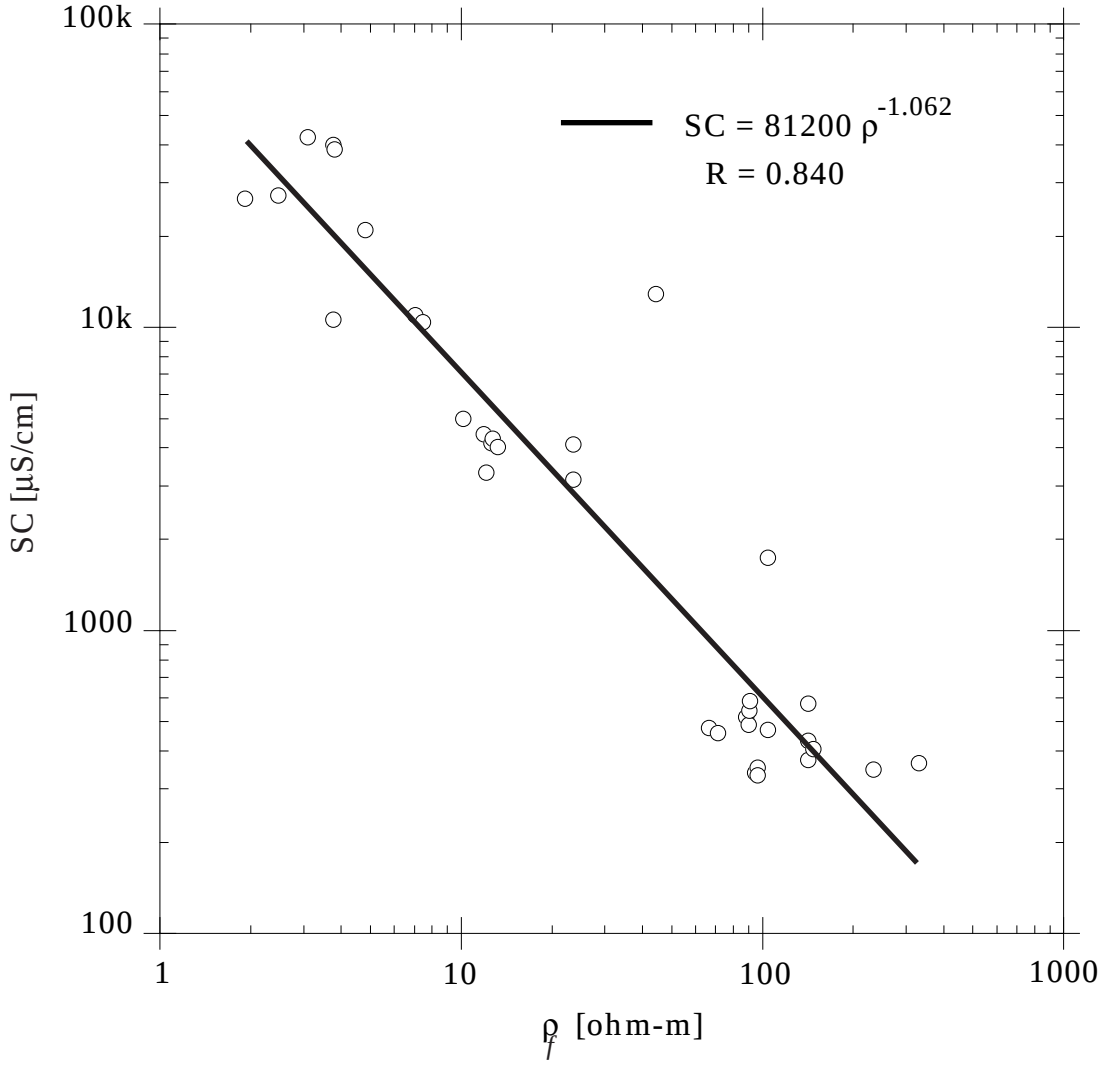

Figure 3 Scatter plot of formation resistivity as a function of water specific conductance from wells in Everglades National Park. The best fit power law through the data is shown.

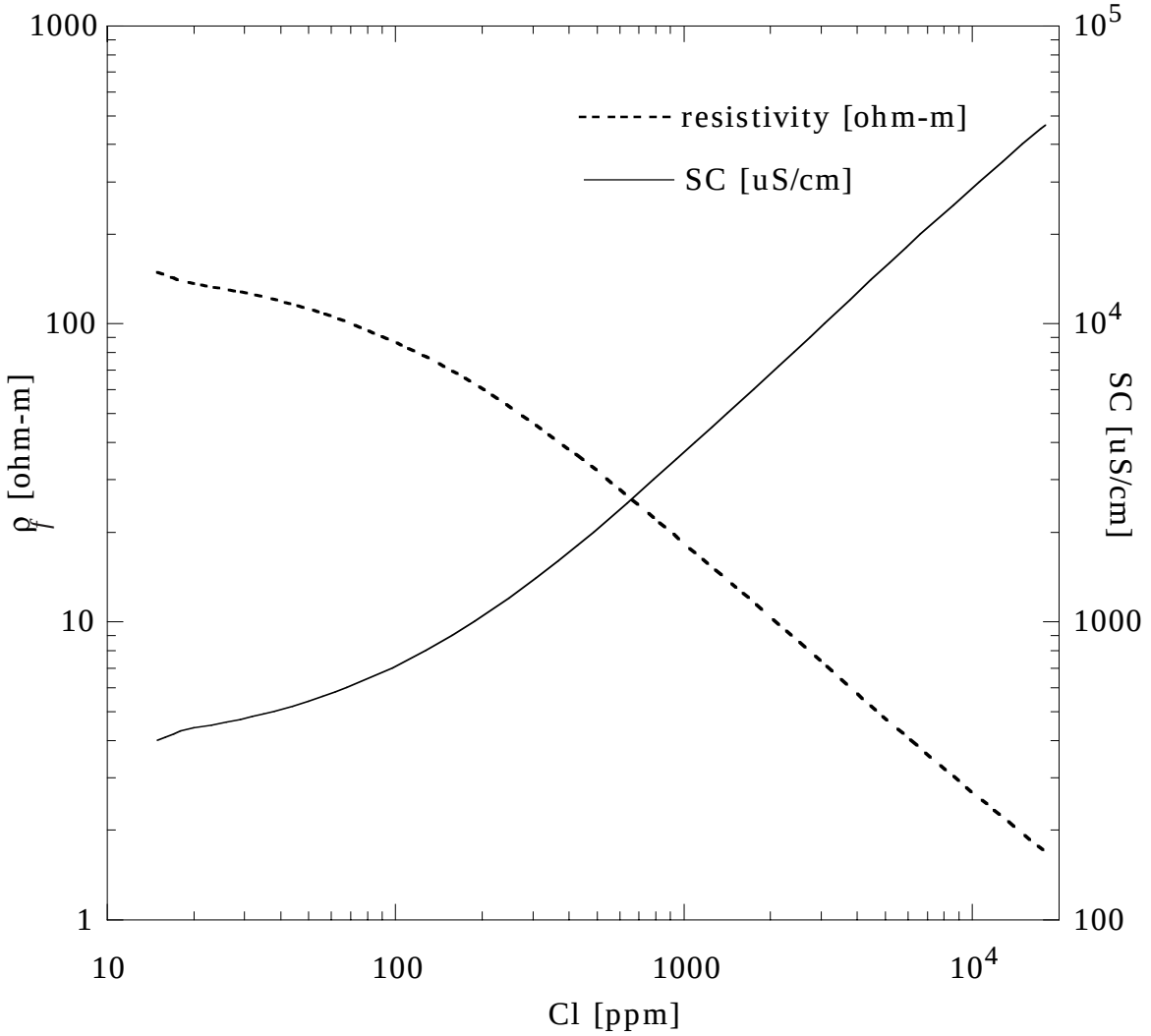

Figure 4 Formation resistivity and water specific conductance as a function of chloride ion concentration.

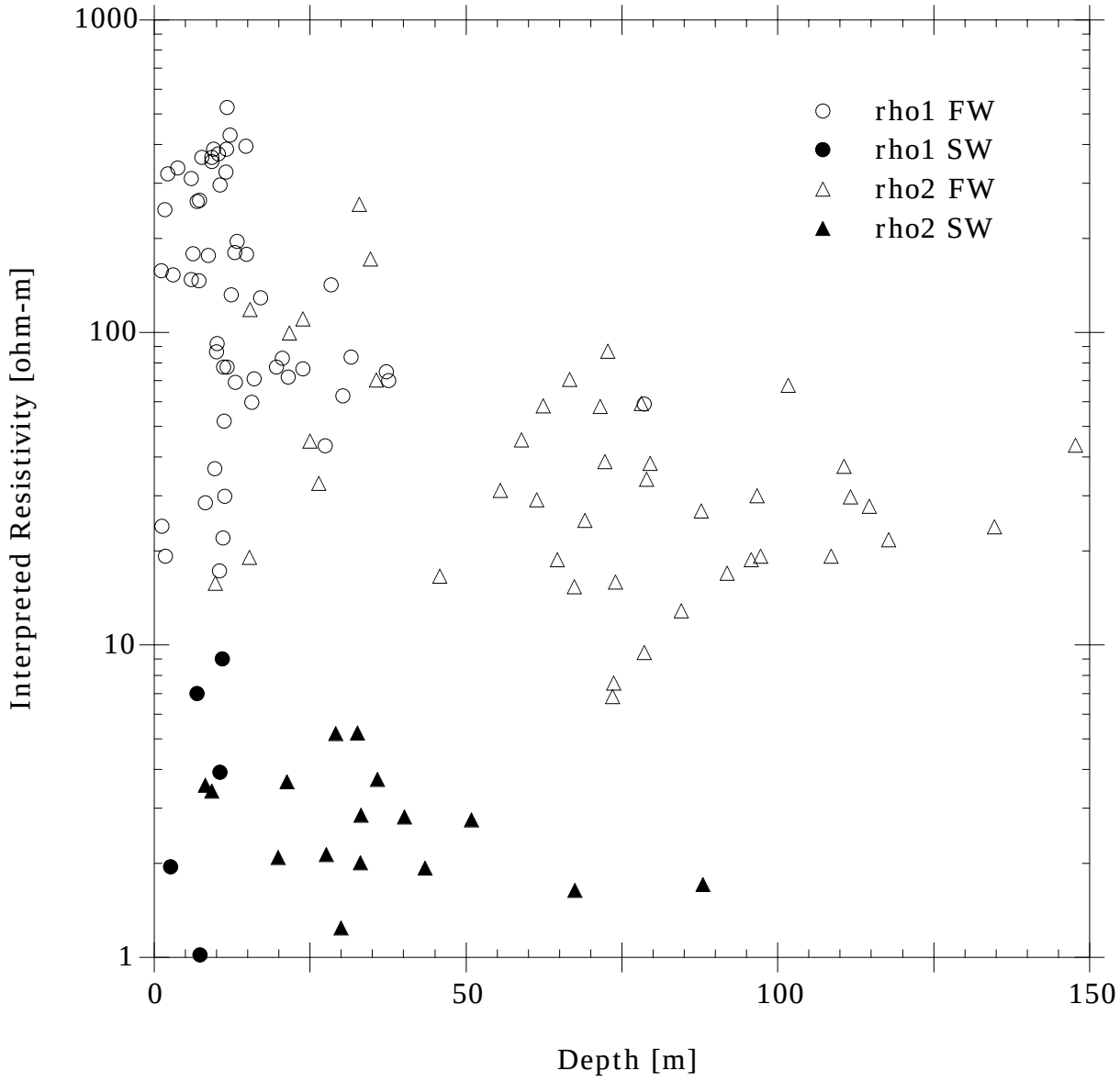

Figure 5 Scatter plot of interpreted layer resistivities as a function of depth to bottom of layer. Resistivities are coded for layer (rho1, rho2) and water quality (FW for freshwater, SW for saltwater).

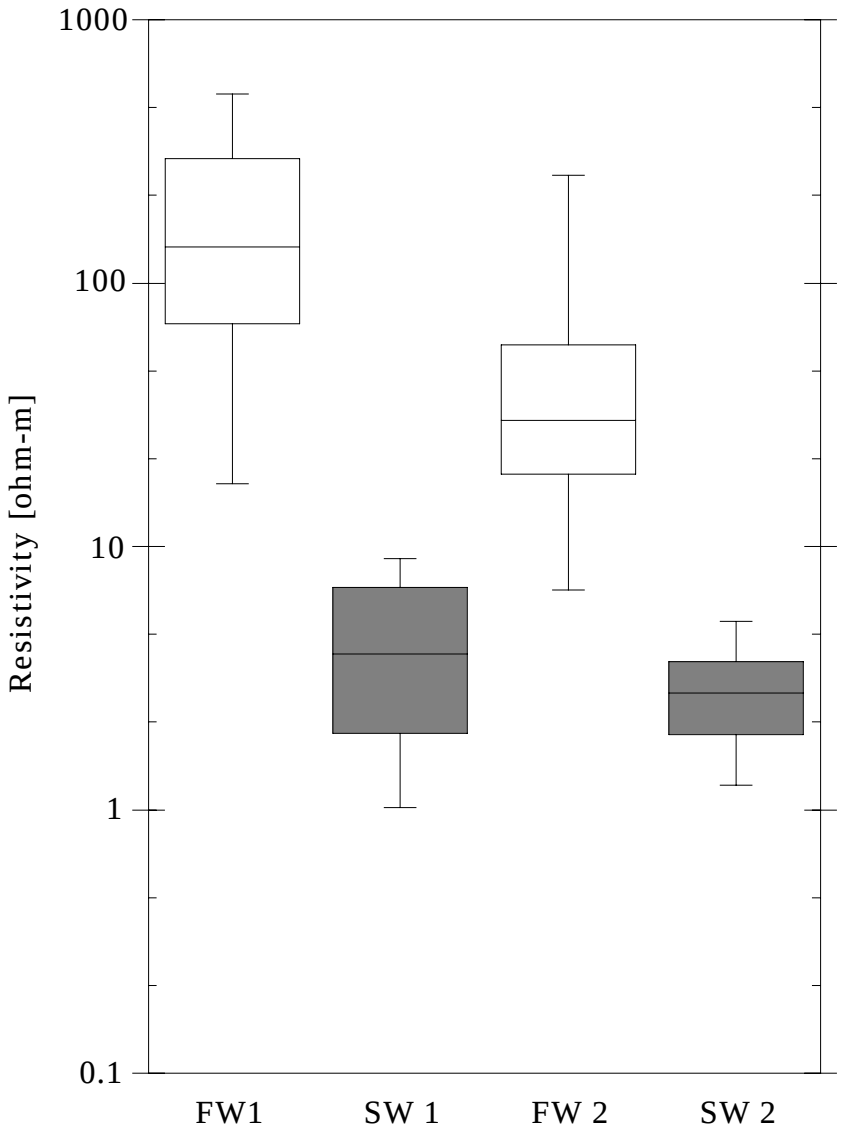

Figure 6 Box plot of interpreted layer resistivities for fresh-water and salt-water saturated zones. FW and SW designate freshwater and saltwater, respectively. The number indicates the TEM model layer.

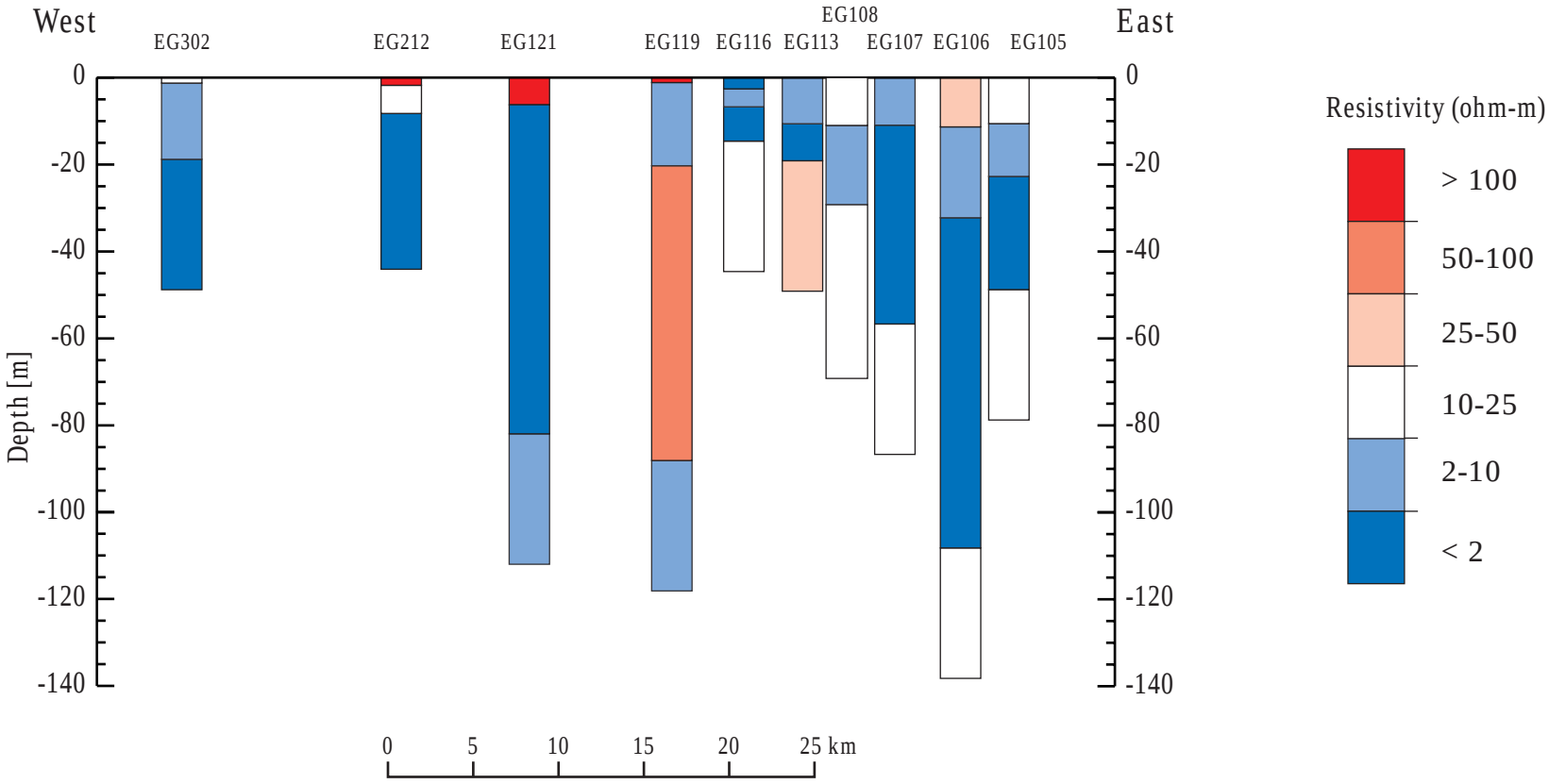

Figure 7 Cross section from soundings along southern edge of study area.

NOTE ON ACROBAT READER LINKS

This document was constructed to be read with Adobe Acrobat Reader. Several types links have been included to make navigation using Acrobat Reader easier.

1. Links to figures are marked in red in the text (for example, Figure 1).
2. Links to plates are marked in blue (for example, Plate 1)
3. The Table of Contents contains unhighlighted links to the various sections of the report. Bookmarks have also been created in Acrobat to assist with navigation.
4. The TEM location symbols in all of the plates are unhighlighted links to the data plots in Appendix 2.
5. The list of data summaries in Appendix 1 are links to the tabular data summaries (for example EG121).
6. The list of data plots in Appendix 2 are linked to the plots (for example EG201).
7. The titles of all of the data plots found in Appendix 2 are unhighlighted links to the associated data summary found in Appendix 1. For example in the first data plot, clicking on the sounding name (EG102) above the apparent-resistivity-time plot will jump to the data summary for the sounding EG102.

APPENDIX 1 DATA SUMMARIES

This appendix contains the measurement parameters (loop size, transmitter current, receiver gain, and receiver coil size), measured apparent resistivity-time data, uncertainty estimates for the measured data, computed best-fit model response, and the interpreted resistivity-depth model in tabular form for all of the TEM soundings. Data for two transmitter repetition frequencies were recorded for each sounding. The various parameters are described below.

1. Sounding: sounding identifier
2. Date: date measurement was made
3. Location: latitude and longitude of measurement point in degree-minutes-seconds.
4. UTM Coord: measurement point location given as kilometers of northing and false easting in UTM zone 17.
5. Comment: descriptive comment on location or measurement
6. TX loop size: length of parallel sides of the transmitter loop (All loops were squares.)
7. RX location: offset of receiver coil from center of transmitter loop (All arrays had the receiver coil at the center of the transmitter loop.)
8. Model: resistivity and layer thickness of best-fit, layered-earth model
9. Fit Error: weighted average of misfit error between measured and computed model response
10. System: TEM system identifier (All measurements were made using a Geonics EM-47.)
11. Freq: repetition frequency of transmitter wave form
12. Data Set Code: code corresponding to the transmitter repetition frequency
13. TX Cur: transmitter current
14. Turn Off: transmitter turnoff time
15. RX Moment: effective area of the receiver coil
16. Gain Setting: gain setting of the Geonics EM-47. (Actual receiver gain is given by $52.1 \cdot 2^{G}$ where G is the gain setting.)
17. Time: time of apparent resistivity measurement after transmitter turnoff
18. rhoa_obs: averaged value of observed apparent resistivity
19. obs_err: estimated uncertainty in the observed apparent resistivity
20. mask: indicator of whether data were used (u), masked (m) from inversion but plotted, or discarded (d) because errors were too large
21. rhoa_cal: computed apparent resistivity from best-fit model